Progress In Electromagnetics Research M, Vol. 48, 155–162, 2016

ISAR Imaging Based on Iterative Reweighted L_p Block Sparse Reconstruction Algorithm

Junjie Feng* and Gong Zhang

Abstract—Sparse signal recovery algorithms can be used to improve radar imaging quality by using the sparse property of strong scatterers. Traditional sparse inverse synthetic aperture radar (ISAR) imaging algorithms mainly consider the recovery of sparse scatterers. However, the scatterers of an ISAR target usually exhibit block or group sparse structure. By utilizing the inherent block sparse structure of ISAR target images, an iterative reweighted $l_p\,(0 < p \leq 1)$ block sparse signal recovery algorithm is proposed to enhance imaging quality in this paper. Firstly, an ISAR imaging signal model is established with the aid of sparse basis, and the imaging is mathematically converted into block reweighted cost function optimization problem. Then, an iterative algorithm is used to solve the reweighted function minimization problem. In each iteration, the weights are updated based on the closed form solution of the previous iteration. The proposed method is effective to exploit the underlying block sparse structures which does not need the prior knowledge of the number of the blocks. Real data ISAR imaging results are provided to verify that the proposed algorithm in this paper can achieve better images than the images obtained by several popular sparse signal recovery algorithms.

1. INTRODUCTION

Inverse synthetic aperture radar (ISAR) has been widely used for targets imaging in both military and civilian fields due to all day and all weather imaging ability [1–3]. High range resolution is achieved by transmitting wideband signals, while high cross-range resolution is obtained by the coherent processing interval. To achieve desirable ISAR imaging, a long coherent processing interval is needed. However, for a long coherent processing interval, the target may move with maneuvering, and the phase of scatterers cannot be approximated as linear function. Then it needs more complex target motion compensation algorithm. At the same time, if the rotation angle is too large, the Radar Cross Section (RCS) of the scatterer may be time varying, which will increase the difficulty of coherent processing. So implementing imaging with limited pulses is meaningful.

Sparse learning has been very popular in signal processing [4–6]. It is a technique proposed to improve signal separation ability using a prior information of sparse property of the signal. By using the sparse signal recovery algorithm, the imaging quality can be improved. This has been successfully shown in SAR imaging [7, 8], ISAR imaging [9, 10], MIMO radar imaging [11, 12].

Most of the current sparse signal recovery radar imaging algorithms only take advantage of the sparsity of the scatterers, but not considering the structure information of the target. In general, the target of ISAR imaging exhibits block sparse structure where nonzero large scatterers occur in clusters. The block sparse structure can be regarded as a continuity form where the nonzero scatterers are continuously located in the imaging region. Analyses have shown that exploiting the inherent block sparse structure not only can make relaxed conditions for exact reconstruction, but also can greatly

Received 15 April 2016, Accepted 24 May 2016, Scheduled 9 June 2016
* Corresponding author: Junjie Feng (fzy028@163.com).
The authors are with Key Laboratory of Radar Imaging and Microwave Photonics, Ministry of Education, College of Electronic and Information Engineering, Nanjing University of Aeronautics and Astronautics, Nanjing 210016, China.

improve the recovery performance. If the structure of the sparse signal is exploited, better recovery performance can be achieved. Several algorithms have been proposed for recovering block sparse signals, such as Block-OMP [13], mixed l_2/l_1 norm minimization [14], model-based CoSaMP [15]. However, these methods need a priori knowledge of the number of the block sparse signals. In many application conditions, the prior information is often unavailable, which restricts their application and performance.

In order to enhance ISAR imaging performance, we reformulate the ISAR imaging into a block sparse signal recovery problem by exploiting the inherent block sparse structure of the target. A novel iterative reweighted l_p algorithm is proposed to recovery block sparse signals. The proposed algorithm does not need the information of the number of blocks. Real data ISAR imaging results show that the proposed algorithm is effective to utilize the potential block sparse structure and can achieve image performance improvement.

2. ISAR IMAGING MODEL

Assume that the translational motion of the target has been completely compensated via conventional methods. So during the coherent processing interval, the radar transmits a linear frequency-modulated signal

$$s(\hat{t}) = \mathrm{rect}\left(\frac{\hat{t}}{T_p}\right)\exp\left[j2\pi\left(f_c\hat{t} + \frac{1}{2}\gamma\hat{t}^2\right)\right] \tag{1}$$

where $\hat{t}$ is the fast time, f_c denotes the carrier frequency, γ the chirp rate, T_P pulse duration, and $\mathrm{rect}(\cdot)$ the rectangle pulse function. The complex echo envelope from the scatterer can be expressed as

$$s(\hat{t}, t) = A \cdot \mathrm{rect}\left(\frac{\hat{t}}{T_p}\right) \cdot \mathrm{rect}\left(\frac{t}{T_a}\right) \cdot \exp\left\{j2\pi\left(\left(\hat{t} - \frac{2R(t)}{c}\right) + \frac{1}{2}\gamma\left(\hat{t} - \frac{2R(t)}{c}\right)^2\right)\right\} \tag{2}$$

where c is the velocity of light, T_a the coherent processing interval, and A the backward scattering amplitude. After the range compression and neglecting the constant, the received signal can be denoted as

$$\begin{aligned} s(\hat{t}, t) &= A \cdot \sin c\left[T_p\gamma\left(\hat{t} - \frac{2(R_0 + y)}{c}\right)\right] \cdot \exp\left[-j4\pi\frac{(R_0 + y)}{\lambda}\right] \\ &\quad \cdot \mathrm{rect}\left(\frac{t}{T_a}\right) \cdot \exp\left[-j2\pi\left(f \cdot t + \frac{1}{2}\beta \cdot t^2\right)\right] \end{aligned} \tag{3}$$

where λ is the wavelength, and $f = 2x\omega/\lambda$, $\beta = 2x\alpha/\lambda$ are Doppler frequency and Doppler rate, respectively. Assuming that the distance unit includes K strong scatterers, the signal in the range cell corresponding to $\tau = 2(R_0 + y)/c$ can be written as

$$y(t) = \sum_{k=1}^{K} x_k \cdot \mathrm{rect}\left(\frac{t}{T_a}\right) \cdot \exp(-j2\pi f_k t) + n\left(t\right) \tag{4}$$

where x_k and f_k are the kth scattering centers' complex amplitude and Doppler frequency, respectively. $n\left(t\right)$ is the additive noise. The time sequence is $t = [1 : N]^T \cdot \Delta t$, $\Delta t = 1/f_r$, being the time interval, and f_r is the pulse repetition frequency. $N = T_a/\Delta t$ is the number of pulses. Δf_d is the Doppler frequency resolution. The sparse Doppler sequence is $f_d = [1 : Q] \cdot \Delta f_d$, $Q = f_r/\Delta f_d$. Q is the number of Doppler units corresponding to Δf_d. So construct the basis matrix as $\Phi = \{\varphi_1, \varphi_2, \ldots, \varphi_q, \ldots, \varphi_Q\}$, $\varphi_q(t) = \exp(-j2\pi f_d(q)t)$, $0 < q \leq Q$. Then the received discrete signal can be rewritten as

$$y = \Phi x + n \tag{5}$$

where x corresponds to the amplitudes of the scatterers.

To estimate x, we can use the following sparse optimization strategy

$$\hat{x} = \arg\min \|x\|_p \ \text{ subject to } \ \|y - \Phi x\|_2 \leq \xi \tag{6}$$

where ξ is a small positive number relating the norm of n. p indicates the l_p norm. The imaging quality depends greatly on reconstruction algorithms. A variety of popular optimization algorithms have been developed to solve Eq. (6), such as smoothed l_0 norm (SL0) algorithm [16] and sparse Bayesian algorithm [17]. In practice, better recovery performance can be obtained if the structure of the sparse signal is exploited. We give a detailed description about the proposed algorithm in the next section.

3. BLOCK SPARSE RECOVERY ISAR IMAGING ALGORITHM

A block sparse signal, where the nonzero coefficients occur in clusters, is an important structured sparsity. A block sparse signal can be stated as follow:

$$x = [\underbrace{x_1, \ldots, x_d}_{x[1]}, \underbrace{x_{d+1}, \ldots, x_{2d}}_{x[2]}, \ldots, \underbrace{x_{N-d+1}, \ldots, x_N}_{x[M]}]^T \tag{7}$$

where $x[i]$ is the ith block with size d, and T is the transpose. In the block partition, the block sparsity means that there are at most $k < M$ non-zero blocks. We aim to estimate the original signal x with unknown cluster structure.

l_2/l_1 minimization strategy was introduced in [18] to solve the block sparse signal reconstruction problem

$$\min_x \sum_{i=1}^{M} \|x[i]\|_2^1 \text{ subject to } \|y - \Phi x\|_2 \leq \tau \tag{8}$$

where τ bounds l_2 norm of the noise.

Although l_1 norm minimization can solve the sparse signal recovery problem, it needs a larger number of measurements for the sparse signal recovery due to its dependency on the magnitude of the block sparse signal. If we can reduce the dependency of Eq. (8) on l_2 norm of the block sparse signal by exploiting a weighting strategy, the reconstruction performance can be improved. So we present the iterative reweighted $l_p\,(0 < p \leq 1)$ norm algorithm for the reconstruction of block sparse signal.

The cost function of Eq. (8) treats signal and noise equally, and we expect to make the utmost efforts to extract signal components and suppress noise at the same time.

The following reweighted l_p minimization is used:

$$\min_{x,\omega} \sum_{i=1}^{M} \frac{\omega_i^{(l)}}{p} \|x[i]\|_2^p \, \|y - \Phi x\|_2 \leq \tau \tag{9}$$

We rewrite Eq. (9) as the following objective function of the unconstrained minimization:

$$\min_{x,\omega} f(x, \omega) = \frac{1}{2\lambda} \|y - \Phi x\|_2^2 + \sum_{i=1}^{M} \frac{\omega_i^{(l)}}{p} \|x[i]\|_2^p \tag{10}$$

where λ is a positive regularization parameter, and $0 < p \leq 1$, $\left\{\omega_i^{(l)}\right\}_{i=1}^{M}$ are a set of block sparse signal weights, which can be considered as free parameters. $\{\cdot\}^l$ denotes the lth iteration.

The first derivative necessary optimality condition for the solution of x is [19]:

$$\frac{\partial f(x, \omega)}{\partial x} = \frac{1}{\lambda}\left(\Phi^H \Phi x - \Phi^H y\right) + W^{-1} x \tag{11}$$

where H is the conjugate transpose.

We define the diagonal weighting matrix W, for the ith block,

$$W_i = \operatorname{diag}\left(\left\{\frac{\left(\|x[i]\|_2^2\right)^{1-\frac{p}{2}}}{\omega_i^{(l)}}\right\}\right) \tag{12}$$

Setting Eq. (11) to zero, the following optimality condition can be obtained:

$$\left(\Phi^H \Phi x - \Phi y\right) + \lambda W^{-1} x = 0 \tag{13}$$

Due to the nonlinearity, there is no straightforward method to solve the above equation. We use an iterative algorithm to estimate the block sparse solution, where the weights in the current iteration are determined based on the estimate of the block signal obtained in the previous iteration.

Suppose that the fixed $W = W^{(l)}$ have been obtained in the lth iteration step, the solution of Eq. (13), set as the $(l+1)$th iteration, then can be obtained as follows:

$$x^{(l+1)} = \left[\Phi^H \Phi + \lambda \left(W^{(l)}\right)^{-1}\right] \Phi^H y \tag{14}$$

We call the proposed block iterative reweighted l_2/l_p minimization algorithm as BIRL2-L_p.

The total algorithm can be summarized as follows.

1) Initialization step:
   (a) Set the iteration number $l \leftarrow 1$ and $\varepsilon \leftarrow \varepsilon_0$;
   (b) Obtain $\hat{x}^{(0)} = \Phi^H y$;
2) While $l < L$ do:
   (a) Update the non-zero weights:
   Determine $\omega_i^{(l+1)} = \frac{1}{\left\|\hat{x}^{(l)}[i]\right\|_2^p+\varepsilon}$,using $\hat{x}^{(l)}$;
   (b) Signal reconstruction
   Obtain $\hat{x}^{(l+1)}$ by using Eq. (14).
   (c) Update ε:
   If $\frac{\left\|\hat{x}^{(l+1)}-\hat{x}^{(l)}\right\|_2}{\left\|\hat{x}^{(l)}\right\|_2} < \sqrt{\frac{\varepsilon}{100}}$, then $\varepsilon \leftarrow \varepsilon/10$;
   (d) $l \leftarrow l+1$.
3) Output $\hat{x}^{(l+1)}$ to be an approximate solution.

For parameter λ, an appropriately chosen parameter which controls the tolerance of noise. Although the best λ may change continuously with respect to noise level, we use the fixed value of λ in the experiments. An appropriate choice of the weights is to make them inversely proportional to the l_2-norm of the blocks. We use the updated weighted values according to the estimate of the solution in the previous iteration. ε is a regularization positive parameter to prevent instability. We can see that if the estimate solution of the ith block in the lth iteration, $\left\|\hat{x}^{(l)}[i]\right\|_2^p$, is small, $\omega_i^{(l+1)}$ will be large. So the blocks with small l_2-norm approach zero. To improve the ability of avoiding undesirable local minimization, we can use a monotonically decreasing sequence for ε instead of a constant in updating the weighting parameters. At the beginning, we can set a relatively large value to ε, then gradually reduce the value by a factor of 10 in the subsequent iterations.

4. SIMULATION RESULTS

4.1. A ISAR Imaging Performance Versus Pulse Numbers

In this simulation, a set of real data of the Yak-42 plane is used to demonstrate the performance of the proposed ISAR imaging algorithm. The parameters of the radar data are listed as follows: the carrier frequency is 10 GHz with signal bandwidth of 400 MHz, and a range resolution is 0.375 m. The pulse repetition frequency is 100 Hz, i.e., 256 pulses are used in this experiment. In order to investigate the role of the pulse number, three different amounts of pulses (16, 32, and 64 pulses) are implemented. The experimental results are compared to those images obtained by some sparse signal recovery methods including BP method [20], SBL method [18], L_1L_0 method [12] and S-method [21]. For BIRL2-Lp algorithm, parameter λ is set to 10^{-3}. We consider two different values of $p = 0.1$, 0.5 for ISAR imaging. The initial value of ε_0 is 10^{-7}. From Fig. 1, it is noticeable that more pulses generate better imagery results. We can see that when the number of pulses is small (e.g., the plus number is 16 or 32), some clutter points of the target are missing, and several weak artificial points are around in the images obtained by BP method. The images obtained by SBL, L_1L_0 and S-method can show most of the strong scatterers. The target images obtained by BIRL2-Lp method using a small amount of

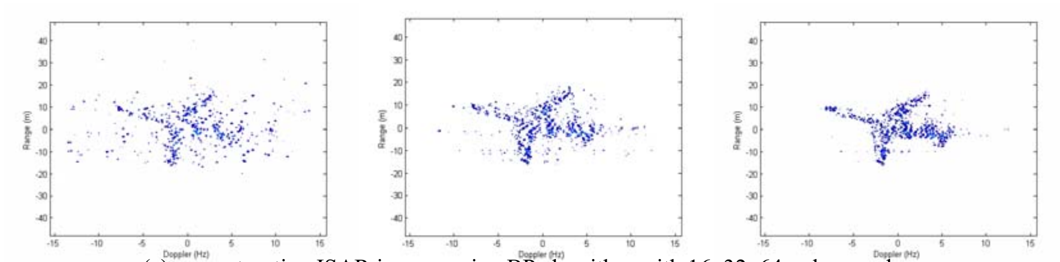

(a) reconstruction ISAR images using BP algorithm with 16, 32, 64 pulse numbers

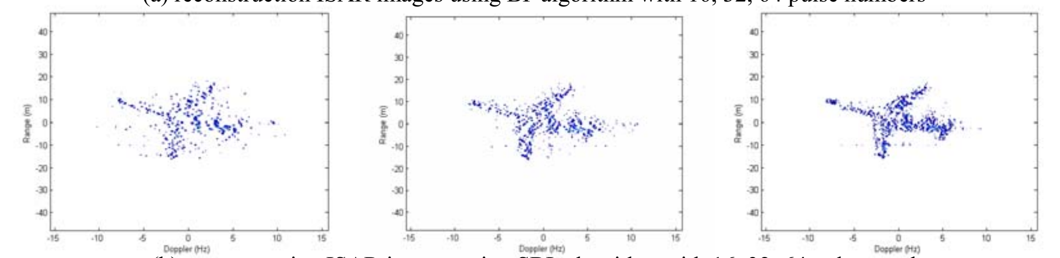

(b) reconstruction ISAR images using SBL algorithm with 16, 32, 64 pulse numbers

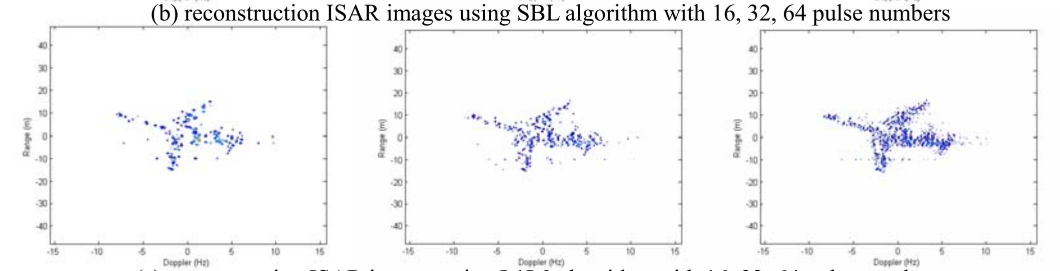

(c) reconstruction ISAR images using L1L0 algorithm with 16, 32, 64 pulse numbers

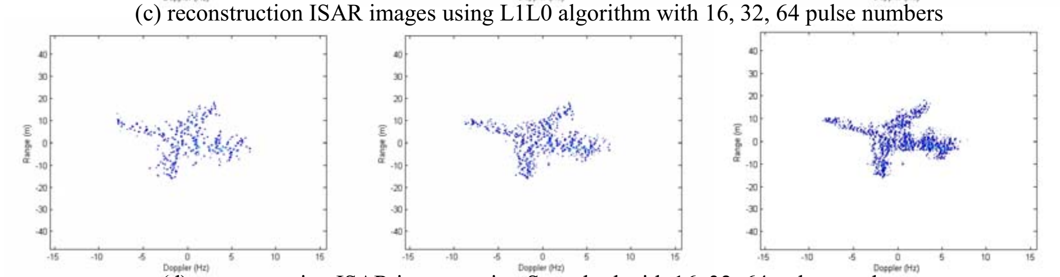

(d) reconstruction ISAR images using S-method with 16, 32, 64 pulse numbers

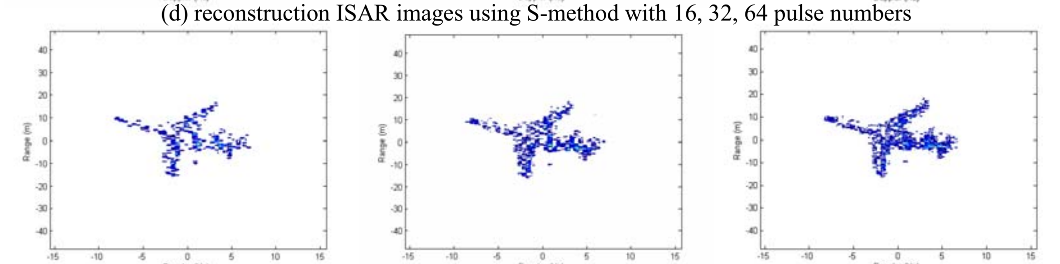

(e) reconstruction ISAR images using BIRL2-Lp (p=0.1) algorithm with 16, 32, 64 pulse numbers

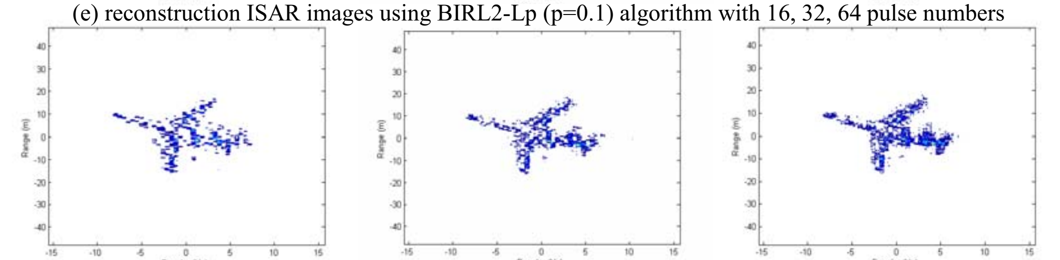

(f) reconstruction ISAR images using BIRL2-Lp (p=0.5) algorithm with 16, 32, 64 pulse numbers

Figure 1. Comparison of the reconstruction ISAR images with different pulse numbers and different algorithms.

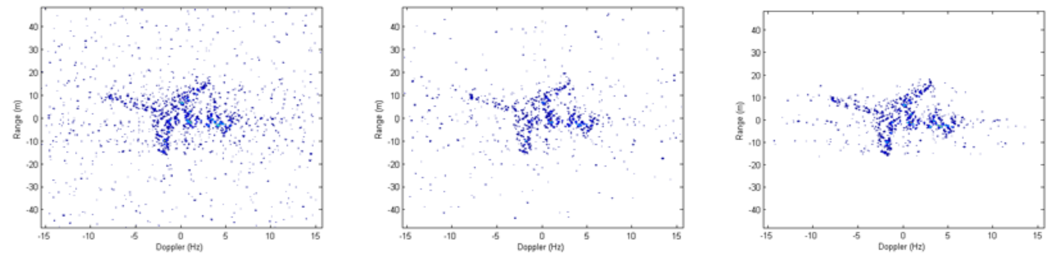

(a) reconstruction ISAR images using BP algorithm with SNR=6dB,8dB,10dB

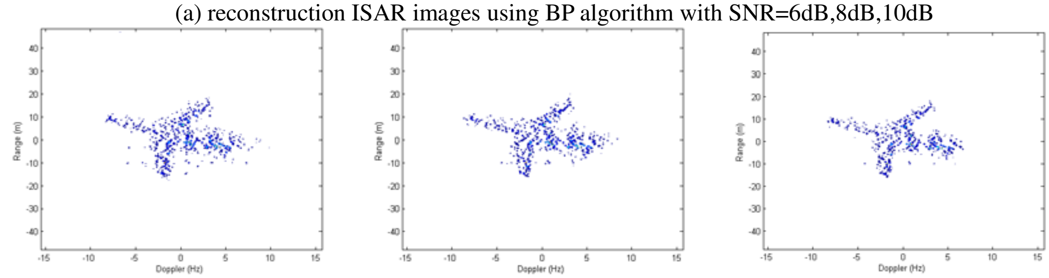

(b) reconstruction ISAR images using SBL algorithm with SNR=6dB,8dB,10dB

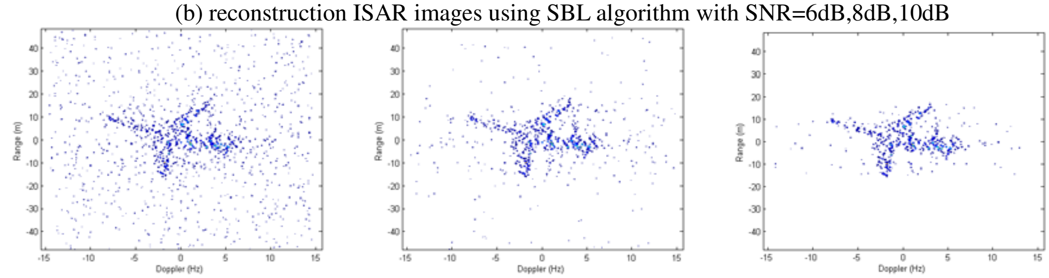

(c) reconstruction ISAR images using L1L0 algorithm with SNR=6dB,8dB,10dB

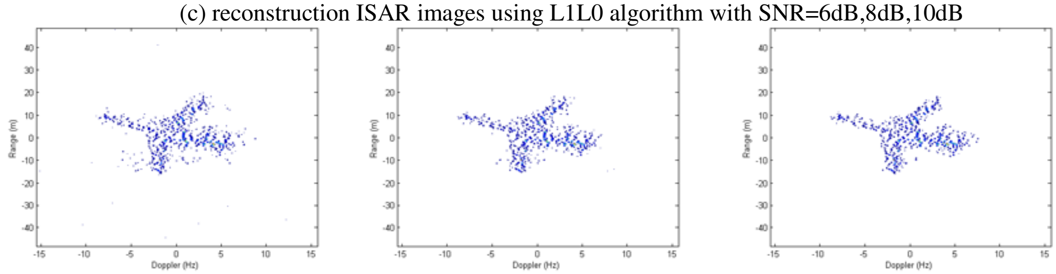

(d) reconstruction ISAR images using S-method with SNR=6dB,8dB,10dB

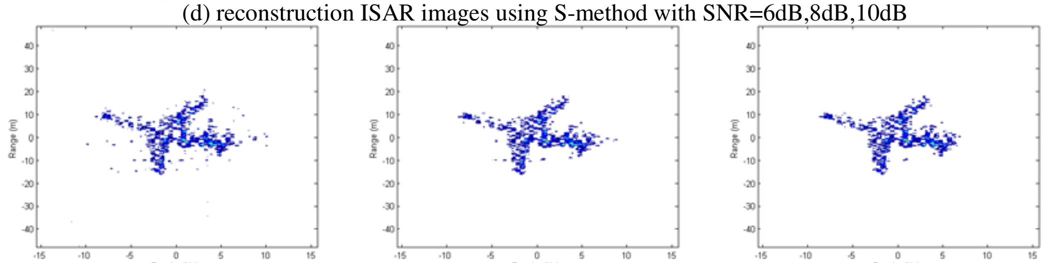

(e) reconstruction ISAR images using BIRL2-Lp algorithm (p=0.1) with SNR=6dB,8dB,10dB

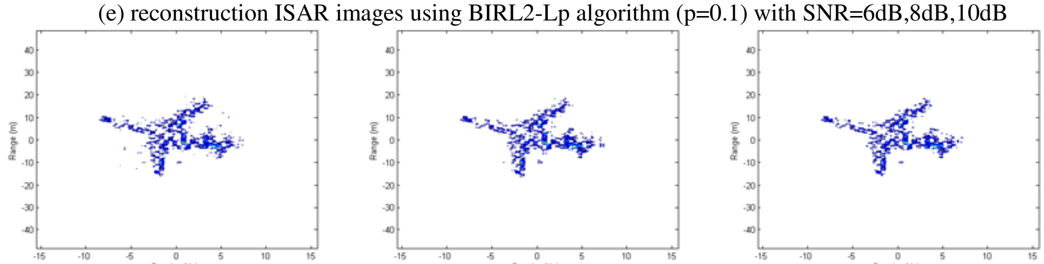

(f) reconstruction ISAR images using BIRL2-Lp algorithm (p=0.5) with SNR=6dB,8dB,10dB

Figure 2. Comparison of the reconstruction ISAR images with different SNRs and different algorithms.

Table 1. Average running times of algorithm.

Algorithm	BP	SBL	L_1L_0	S-method	BIRL2-Lp
Run Time (sec)	136	243	129	65	86

pulse are satisfactory. The proposed algorithm generates better visual and more intensive ISAR images than the images obtained by other methods. The average running times of different algorithms are also provided when the pulse number is 32, and p is set to 0.1 in Table 1. The results are averaged over 100 independent runs. The running time of BIRL2-Lp method is shorter than that of BP method, SBL method and L_1L_0 method, which is useful for real-time ISAR imaging.

4.2. ISAR Imaging Performance Versus Noise

To test the robustness of the proposed algorithm, complex valued Gaussian noise is added to the real data to generate different SNRs. The imaging results obtained by BP, SBL, L_1L_0, S-method and BIRL2-Lp method using a constant amount of pulses and different SNRs are given in Fig. 2. The SNRs are 6 dB, 8 dB, 10 dB, respectively. It is noticeable that the reconstructed images of BP method and L_1L_0 method are obscure.

The imaging results of BP method and L_1L_0 method are obscure. There are many artificial points outside the target region. The SBL method, S-method and BIRL2-Lp method have superior robustness to other methods. The ISAR images recovered by BIRL2-Lp method extract more proper scattering centers of the target and have decent performance in the noisy case.

5. CONCLUSIONS

The traditional ISAR imaging algorithms based on sparse signal recovery only consider the sparsity of the scatterers. They do not exploit the inherent structure information of the target in the imaging region. A novel ISAR imaging algorithm based on iterative reweighted block sparse signal recovery is proposed to obtain an enhanced image by exploiting the block sparse structure of target in this paper. The real data experiments show that the proposed algorithm can improve ISAR imaging quality and has superior robustness.

ACKNOWLEDGMENT

This work was supported by the National Natural Science Foundation of China under grant (No. 61471191).

REFERENCES

1. Jung, J. H., K. T. Kim, S. H. Kim, and S. H. Park, "An efficient ISAR imaging method for multiple targets," *Progress In Electromagnetics Research*, Vol. 146, 133–142, 2014.
2. Kim, D., D. Seo, and H. Kim, "Efficient classification of ISAR images," *IEEE Transaction on Antennas and Propagation*, Vol. 53, No. 5, 1611–1621, 2005.
3. Wang, H., Y. Qun, M. Xing, and S. Zhang, "ISAR imaging via sparse probing frequencies," *IEEE Geosci. Remote Sens. Lett.*, Vol. 8, No. 3, 451–455, 2011.
4. Needell, D. and R. Vershynin, "Uniform uncertainty principle and signal recovery via regularized orthogonal matching pursuit," *IEEE Journal of Selected Topics in Signal Processing*, Vol. 4, No. 9, 317–334, 2009.
5. Tropp, J. A. and A. C. Gilbert, "Signal recovery from random measurements via orthogonal matching pursuit," *IEEE Transactions on Information Theory*, Vol. 53, No. 12, 4655–4666, 2007.
6. Demba, B., B. Behtash, and L. Patrick, "Convergence and stability of iteratively re-weighted least squares algorithms," *IEEE Trans. Signal Process.*, Vol. 62, No. 1, 183–159, 2014.

7. Zhang, X. Z., J. H., Qin, and G. J. Li, "SAR Target classification using bayesian compressive sensing with scattering centers features," *Progress In Electromagnetics Research*, Vol. 136, 385–407, 2013.
8. Cetin, M., I. Stojanovic, O. Onhon, K. Varshney, S. Samadi, W. C. Karl, and A. S. Willsky, "Sparsity-driven synthetic aperture radar imaging," *IEEE Signal Processing Magazine*, Vol. 31, No. 4, 27–40, 2014.
9. Liu. J., X. Li, S. Xu, and Z. Zhuang, "ISAR imaging of non-uniform rotation targets with limited pulses via compressed sensing," *Progress In Electromagnetics Research B*, Vol. 41, 285–305, 2012.
10. Zhang, L., M. Xing, C. W. Qiu, et al., "Achieving higher resolution isar imaging with limited pulses via compressed sampling," *IEEE Geosci. Remote Sens. Lett.*, Vol. 6, No. 3, 57–571, 2009.
11. Ma, C. Z., T. S. Yeo, Y. B. Zhao, and J. J. Feng, "MIMO radar 3D imaging based on combined amplitude and total variation cost function with sequential order one negative exponential form," *IEEE Trans. Image Process.*, Vol. 23, No. 5, 2168–2183, 2014.
12. Tan, X., W. Roberts, J. Li, and P. Stoica, "Sparse learning via iterative minimization with application to MIMO radar imaging," *IEEE Trans. Signal Process.*, Vol. 59, No. 3, 1088–1101. 2011.
13. Eldar, Y., P. Kuppinger, and H. Bolcskei, "Block-sparse signals: Uncertainty relations and efficient recovery," *IEEE Trans. Signal Process.*, Vol. 58, No. 6, 3042–3054, 2010.
14. Eldar, Y. and M. Mishali, "Robust recovery of signals from a structured union of subspaces," *IEEE Transactions on Information Theory*, Vol. 55, No. 1, 5302–5316, 2009.
15. Baraniuk, R. G., V. Cevher, M. F. Duarte, and C. Hegde, "Model-based compressive sensing," *IEEE Transactions on Information Theory*, Vol. 56, No. 4, 1982–2001, 2010.
16. Mohimani, H., M. Babaie-Zadeh, and C. Jutten, "A fast approach for overcomplete sparse decomposition based on smoothed l_0 norm," *IEEE Trans. Signal Process.*, Vol. 57, No. 1, 289–301, 2009.
17. Wipf, D. P. and B. D.Rao, "Sparse Bayesian learning for basis selection," *IEEE Trans. Signal Process.*, Vol. 52, No. 8, 2153–2164, 2004.
18. Stojnic, M., F. Parvaresh, and B. Hassibi, "On the reconstruction of block-sparse signals with an optimal number of measuremets," *IEEE Trans. Signal Process.*, Vol. 57, No. 8, 3075–3085, 2009.
19. Gong, P. C. and Z. H. Shao, "Target estimation by iterative reweighted l_q minimization for MIMO radar," *Signal Processing*, Vol. 101, 35–41, 2014.
20. Chen, S., D. Donoho, and M. Saunders, "Atomic decomposition by basis pursuit," *SIAM Review*, 129–159, 2001.
21. Stankovic, L., "On the ISAR image analysis and recovery with unavailable or heavily corrupted data," *IEEE Transactions on Aerospace and Electronic Systems*, Vol. 51, No. 3, 2093–2106, 2015.